

We are IntechOpen, the world's leading publisher of Open Access books Built by scientists, for scientists

6,900

Open access books available

185,000

International authors and editors

200M

Downloads

Our authors are among the

154

Countries delivered to

TOP 1%

most cited scientists

12.2%

Contributors from top 500 universities



WEB OF SCIENCE™

Selection of our books indexed in the Book Citation Index
in Web of Science™ Core Collection (BKCI)

Interested in publishing with us?
Contact book.department@intechopen.com

Numbers displayed above are based on latest data collected.
For more information visit www.intechopen.com



Modelling and Control of Narrow Tilting Vehicle for Future Transportation System

Yaxing Ren

Abstract

The increasing number of cars leads traffic congestion and parking problems in urban area. Small electric four-wheeled narrow tilting vehicles (NTV) have the potential to become the next generation of city cars. However, due to its narrow width, the NTV has to lean into corners like two-wheeled vehicles during a turn. It is a challenge to maintain its roll stability to protect it from falling down. This chapter aims to describe the development of NTV and drive assistance technologies in helping to improve the stability of an NTV in turning. The modelling of an NTV considers the dynamics of the tyres and power train of the vehicle. A nonlinear tilting controller for the direct tilting control mechanism is designed to reduce the nonlinear behaviour of an NTV operating at different vehicle velocities. In addition, two torque vectoring based torque controllers are designed to reduce the counter-steering process and improve the stability of the NTV when it turns into a corner. The results indicate that the designed controllers have the ability to reduce the yaw rate tracking error and maximum roll rate. Then riders can drive an NTV easily with the drive assistance system.

Keywords: modelling, stability control, nonlinear control, torque vectoring, drive assistance system, narrow tilting vehicle

1. Background

Vehicle is one of the most widely used transportation in people's daily life. Due to the greenhouse gas emission problem of traditional cars, the development of electric vehicles received great attention in recent years. However, in urban area, the increasing number of cars causes the traffic congestion problems and limit parking places. Because of these issues, small narrow commuter vehicles are expected to become a new generation of city cars [1, 2]. In the UK, some researches have been done in the past years, such as the CLEVER Project [3–5] and RESOLVE Project [6, 7], which developed two prototype vehicles as shown in **Figure 1** [8]. This kind of vehicles are also called narrow tilting vehicles (NTVs) have just half the width of a conventional car like a motorcycle but have four wheels like a car. This makes an NTV a convergence of a car and a motorcycle that makes it integrate the features and advantages of them.

The conventional four-wheel vehicles is wide that have enough roll stiffness to balance the roll stability by its own suspension structure. But the NTV has no such roll stiffness and have to lean into corners during turning [3, 9], as shown in



Figure 1.
Two demonstrators of narrow tilting vehicle developed in the RESOLVE Project [8].

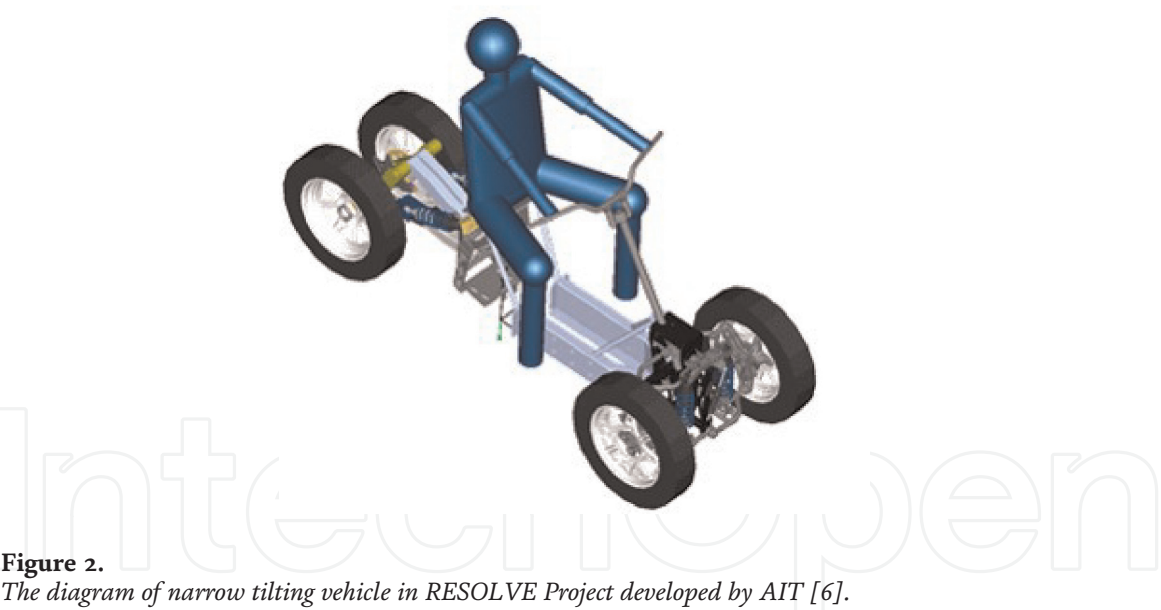


Figure 2.
The diagram of narrow tilting vehicle in RESOLVE Project developed by AIT [6].

Figure 2. This is a challenge to the roll stability of NTV and need to be maintained by experienced riders. The purpose of the vehicle design is not only driven by experienced riders but also new riders. Thus, the autonomous drive assistance system is required to improve its roll stability [10–12].

In riding a motorcycle, the rider can lean the motorcycle into a corner by shifting his own weight. But this is not available in riding an NTV as the weight of a human body is much lighter than that of the vehicle. Thus, in riding an NTV, the rider has to act on the throttle with counter-steering process to balance the vehicle in a turn [3, 9]:

- the rider provides a counter-steering on the throttle on an opposite direction;
- the counter-steering provides the opposite lateral force;

- the lateral force rolls the vehicle into the expected side;
- the rider then turns the steering back to the expected direction at an appropriate moment; and
- the vehicle stops rolling down and yaws to the expected route.

It shows that the riders of NTVs have to be very experienced in balancing the vehicle and following the path simultaneously. The NTV can be in different tilting states, such as straight on, turning, accelerating turn, oversteer/understeer and highsider, as shown in **Figure 3**. However, the next generation vehicles are expected to be easy-driving to low-experienced riders. A drive assistance system can help new riders in balancing the vehicle and the riders only need to focus on the path in the riding. This leads the development of an autonomous drive assistance system for NTV.

To improve the tilting stability, the common solution is to design the active tilting control via installing additional mechanisms. The two main tilting methods are the steering tilt control (STC) and the direct tilt control (DTC) on different mechanisms [13, 14], as shown in **Figure 4**. The STC directly controls the steering angle of front wheel to autonomously complete the tilting process as an experienced rider for stabilising the vehicles, while the DTC provides additional torque to lean the vehicle to the expected corners.

The STC system is efficient at high speed but performs worse at the standstill or very low speeds. In slippery road conditions, the performance of using STC is even worse [15]. The DTC based mechanism slightly simplifies these control problems with an additional control input from a separate tilt actuator [16]. But the DTC

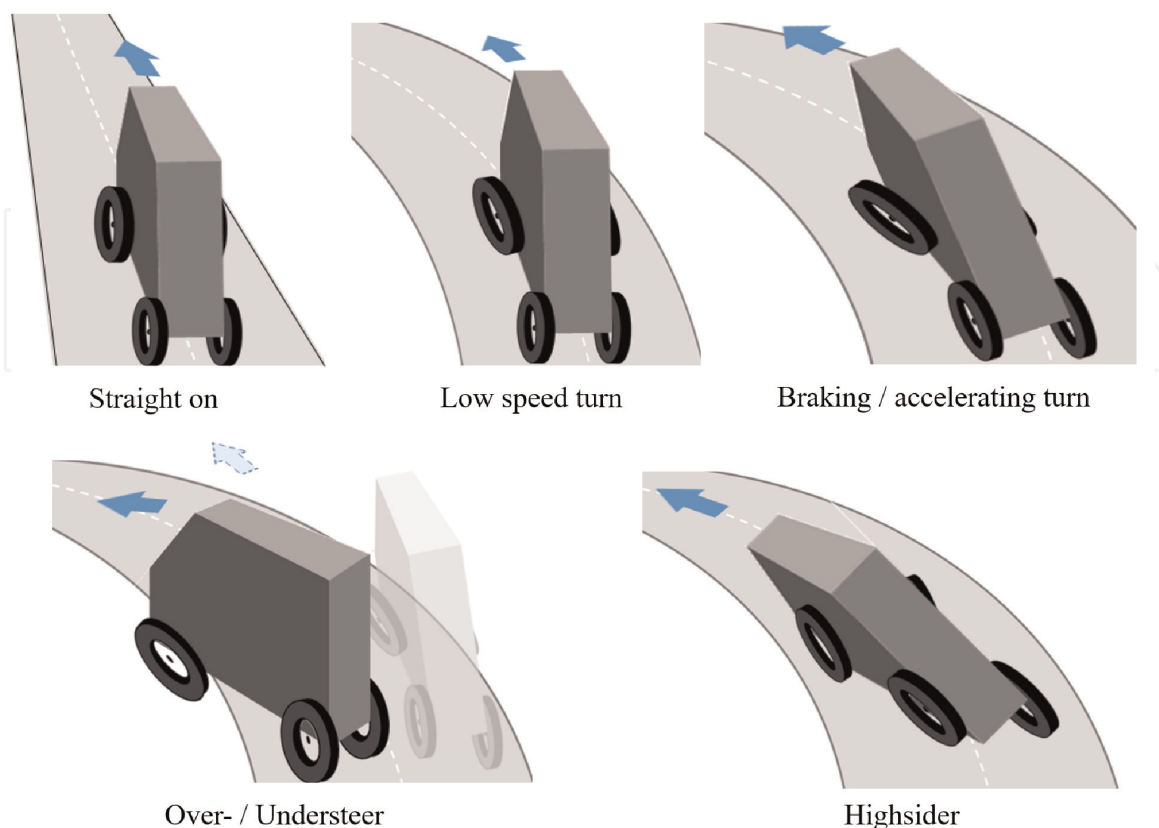


Figure 3.
Tilting states of NTV.

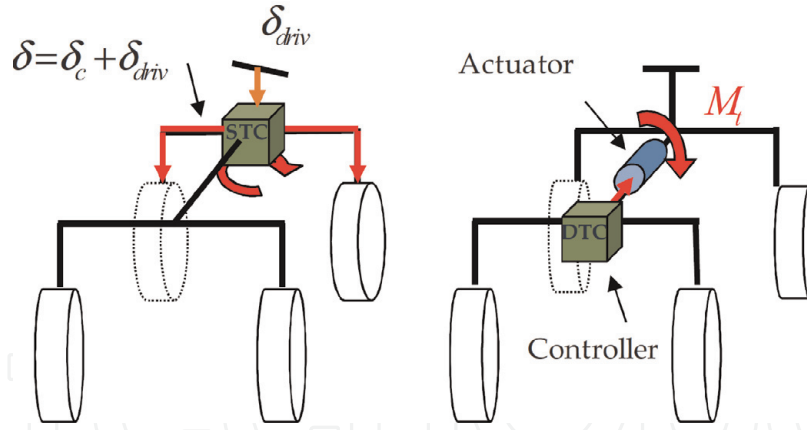


Figure 4.
The STC and DTC tilting mechanisms of NTV [10].

system requires high tilting motion at high vehicle speed and has risk to cause the vehicle oscillations. In addition, the delayed vehicle response speed could reduce the performance of tilting motion. Thus, it requires highly sophisticated loop control algorithms adapting to different loads and driving conditions [16]. The combination of STC and DTC in dual mode switching strategies is available to reduce their drawbacks. But such approaches have obvious discontinuous behaviour during the mode switching [4, 14, 17].

Several studies focused on the control approach design in driving the DTC actuator, including linear SISO control approaches to provide tilt torque from a given combination of vehicle information [2, 18], model-based control methods to decouple the longitudinal and lateral dynamics in vehicle response [5, 19, 20], and nonlinear control solutions to compensate the nonlinear behaviour of NTVs based on the accurate vehicle model [20, 21].

On the other side, the torque vectoring (TV) technology is able to improve the vehicle cornering response and potential to improve the handling performance of a vehicle [22]. The left-right TV technique was proposed in [23] aiming to distribute the driving and braking forces on left and right wheels in a wheel-individual vehicle. The control allocation criteria were verified sensitive to electric motor drive parameters in performance comparison [24]. The maximum vectoring torque limit was determined in [25] and desired traction force and yaw moment were mapped in [26]. The TV approach was optimised to improve the yaw moment distraction performance in [27] and the stability of NTV under expected environmental conditions in [28]; the lateral stability in cornering was enhanced by optimal TV approach to maximise the vehicle velocity in [29]; and minimised the power losses of TV to improve the battery efficiency [30].

In these approaches, the TV method is used as an assistant torque mainly for improving the performance of vehicle yaw turn and enhancing the lateral stability. The yaw moment on a vehicle can also affect the roll stability and it is more sensitive to an NTV. The conventional TV methods and their optimisation may not be suitable for both yaw and roll stability enhancement. Thus, the roll stability maintenance of using the TV technology needs to be paid more attention in an NTV.

This chapter first designs a nonlinear tilting controller for DTC-based NTVs without the dependence of an accurate vehicle model to improve the performance of DTC from low speed to high speed. In addition, this chapter develops the TV technology based drive assistance system to maintain the roll dynamics of NTV in cornering. Both approaches are developed to assist the rider in turning an NTV and improve the roll stability of the vehicle. As a result, both the new rider and experienced rider can drive the NTV easily.

2. Mathematical model of four-wheel vehicle dynamics

The basic model of NTV was proposed in 1990s for the two or three wheeled tilting vehicles from the simplified bicycle geometric model [17, 31, 32]. The model considers the vehicle body dynamic only and the wheels are assumed with light weighting and not leaning with the vehicle body. The University of Minnesota proposed the nonlinear NTV model with wheel dynamics considering the distribution force on each wheel [16, 20, 33]. The University of Bath proposed a five DoF nonlinear model of NTV and wheel dynamics [3–5]. On the other hand, due to the contacts between road surface and tyre significantly affects the friction force of wheel dynamics, the tyre longitudinal slip can be combined into the wheel dynamic in the NTV model. This section will discuss the detailed NTV model to describe the dynamics of traction force transferred from tyre to vehicle body and simplified single-track vehicle model for controller design.

2.1 Wheel dynamics

As seen in the wheel dynamic model in **Figure 5**, the wheel speed ω_{ij} describes the power transfer from rear-wheel-drive wheel hub to road. In four-wheeled vehicle, the wheels of front left, front right, rear left, and rear right wheels are represented as $ij \in \{fl, fr, rl, rr\}$. The traction torque T_{rj} is applied on rear left and rear right wheels and the brake torque $T_{brk,i}$ are applied on the centre of all wheels. The longitudinal force $F_{l,ij}$ is the force to drive the wheels at the contact point between tyre and road surface.

The dynamics of wheel speeds are represented as [12, 34]:

$$\dot{\omega}_{fj} = \frac{-T_{brk,f} - R_f F_{l,fj}}{J_{fj}} \quad (1)$$

$$\dot{\omega}_{rj} = \frac{T_{rj} - T_{brk,r} - R_r F_{l,rj}}{J_{rj}} \quad (2)$$

where J_{ij} is the wheels' inertia around the wheel with the radius R_i .

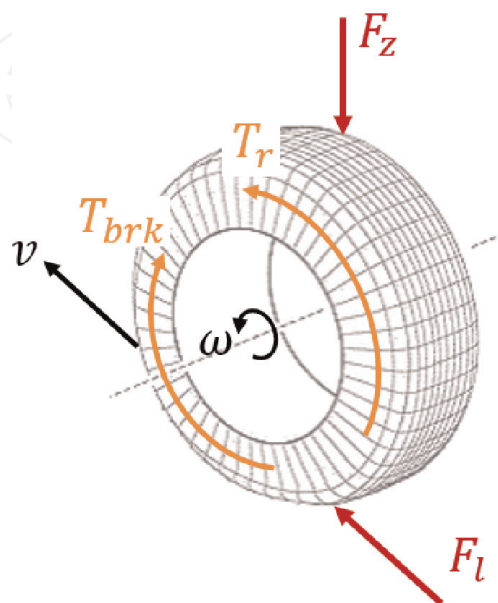


Figure 5.
 Wheel dynamic model.

The longitudinal force can be described as a function of friction coefficient μ_{ij} and tyre longitudinal slip $s_{l,ij}$ as

$$F_{l,ij} = F_{z,ij} \cdot \mu_{ij}(s_{l,ij}) \quad (3)$$

where the tyre longitudinal slip $s_{l,ij}$ can be described based on the vehicle velocity v and vehicle side-slip angle β as:

$$s_{l,ij} = \frac{R_i \omega_{ij} - v \cos \beta}{\max(R_i \omega_{ij}, v \cos \beta)} \quad (4)$$

which describes the longitudinal slip of both acceleration and braking conditions, as shown in **Figure 6**.

The tyre characteristics of friction coefficient μ_{ij} are modelled by the *magic tyre formula* as [35].

$$\mu_{ij}(x_{ij}) = D \cdot \sin \left\{ C \arctan \left[B(1 - E) \cdot x_{ij} + E \arctan (B \cdot x_{ij}) \right] \right\} \quad (5)$$

where B , C , D and E are the parameters to determine the friction coefficient of tyre, the input x_{ij} can be either longitudinal slip $s_{l,ij}$ to calculate the longitudinal slip friction coefficient or lateral slip angle α_{ij} to calculate the side slip friction coefficient [36]. An example of the longitudinal tyre characteristics of friction coefficient with wheel slip ratio on typical roads of dry, wet, snow and iced conditions, as shown in **Figure 7**.

The vertical load $F_{z,ij}$ of each wheel can be calculated by

$$F_{z,fl} = m \left(\frac{l_r}{l} g - \frac{h}{l} a_x \right) \left(\frac{1}{2} - \frac{h}{b_f} \frac{a_y}{g} \right) \quad (6)$$

$$F_{z,fr} = m \left(\frac{l_r}{l} g - \frac{h}{l} a_x \right) \left(\frac{1}{2} + \frac{h}{b_f} \frac{a_y}{g} \right) \quad (7)$$

$$F_{z,rl} = m \left(\frac{l_f}{l} g + \frac{h}{l} a_x \right) \left(\frac{1}{2} - \frac{h}{b_r} \frac{a_y}{g} \right) \quad (8)$$

$$F_{z,rr} = m \left(\frac{l_f}{l} g + \frac{h}{l} a_x \right) \left(\frac{1}{2} + \frac{h}{b_r} \frac{a_y}{g} \right) \quad (9)$$

where m is the lumped mass of vehicle itself and rider; g is the gravitational constant; l is the distance of wheelbases consisting l_f and l_r , which represent the distance from the centre of gravity (COG) to front axles and rear axles, respectively; h indicates the vehicle height that is measured from the road surface to the COG of the vehicle; b_f and b_r are the track of front and rear axle; a_x and a_y are the acceleration of vehicle in x-axis and y-axis of the vehicle-fixed coordinate system.

The tyre sideslip force is presented by the magic tyre formula in (5) as

$$F_{s,ij} = F_{z,ij} \cdot \left[\mu_{ij}(\alpha_{ij}) + \lambda_{st} \theta \right] \quad (10)$$

where θ is the lean angle of wheels, which is the same as lean angle of vehicle, and λ_{st} is the camber stiffness coefficient of wheels. The wheel lateral slip angle α_{ij} represents the angle between the longitudinal axis of wheel and its velocity forward direction. The lateral slip angle can be presented as

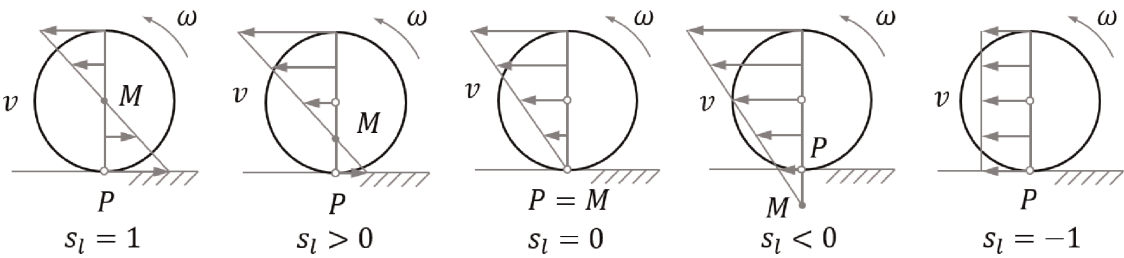


Figure 6.
 Wheel slip ratio at different wheel rotating conditions.

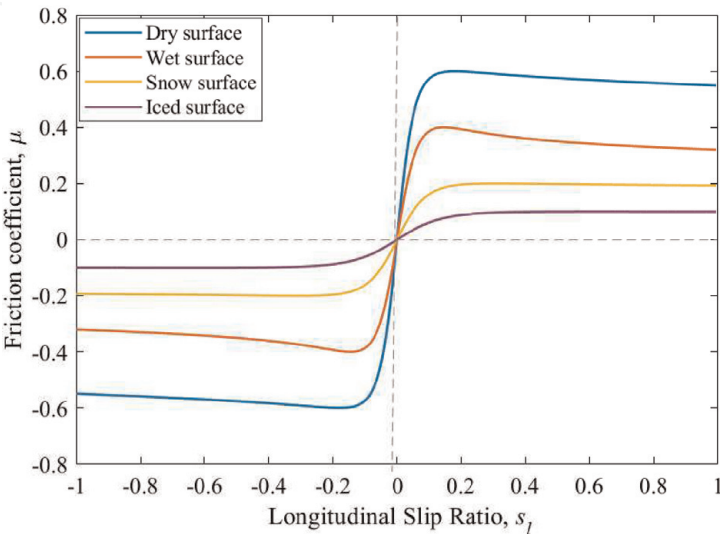


Figure 7.
 Longitudinal tyre characteristics of variable friction coefficient with longitudinal slip ratio.

$$\alpha_{fj} = \delta - \arctan \left(\frac{v \sin \beta + l_f \dot{\varphi}}{v \cos \beta} \right) \tag{11}$$

$$\alpha_{rj} = - \arctan \left(\frac{v \sin \beta - l_r \dot{\varphi}}{v \cos \beta} \right) \tag{12}$$

where δ is steering angle of front wheels and $\dot{\varphi}$ is the yaw rate of vehicle.
 The traction force and lateral force of wheels in vehicle-fixed coordinate system, $F_{x,fj}$, $F_{y,fj}$, $F_{x,rj}$ and $F_{y,rj}$, can be presented by the transformation

$$F_{x,fj} = F_{l,fj} \cos \delta - F_{s,fj} \sin \delta \tag{13}$$

$$F_{y,fj} = F_{l,fj} \sin \delta + F_{s,fj} \cos \delta F_{x,rj} = F_{l,rj} \tag{14}$$

$$F_{y,rj} = F_{s,rj} \tag{15}$$

2.2 Vehicle dynamics

The vehicle dynamic of an NTV is the combination of a vehicle model and a bicycle model. In modelling an NTV system, the vehicle and its rider (and passenger) can be seen as a single mass model. The vehicle model of narrow tilting vehicle includes the velocity dynamic, side-slip angle dynamic, yaw dynamic and roll dynamic [30]. The geometry model of an NTV is shown as in **Figure 8**. The vehicle motion dynamics can be described by the vehicle velocity v and the vehicle side-slip

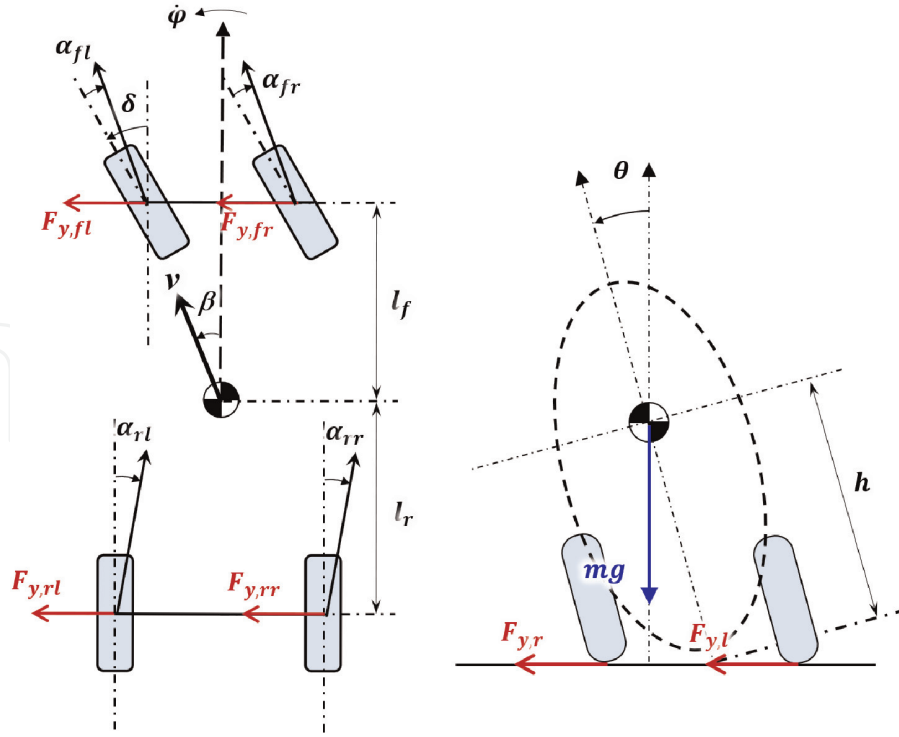


Figure 8.
Geometry of a narrow tilting vehicle.

angle β , which is defined as the angle between v and the vehicle longitudinal axis x . Their dynamics can be represented by

$$\dot{v} = \frac{1}{m} \left(\cos \beta \sum_{ij} F_{x,ij} + \sin \beta \sum_{ij} F_{y,ij} - F_{\text{res}} \right) \quad (16)$$

$$\dot{\beta} = \frac{1}{mv} \left(\cos \beta \sum_{ij} F_{y,ij} - \sin \beta \sum_{ij} F_{x,ij} \right) - \dot{\varphi} \quad (17)$$

where F_{res} represents the force of driving resistance.

The vehicle acceleration in x- and y-axis a_x and a_y are presented by v , β , φ and their differentials as

$$a_x = \dot{v} \cos \beta - v(\dot{\beta} + \dot{\varphi}) \sin \beta \quad (18)$$

$$a_y = \dot{v} \sin \beta + v(\dot{\beta} + \dot{\varphi}) \cos \beta \quad (19)$$

The vehicle yaw motion in the second-order differential equation is represented as

$$\ddot{\varphi} = \frac{1}{I_z} \left[l_f (F_{y,fl} + F_{y,fr}) - l_r (F_{y,rl} + F_{y,rr}) + \frac{b_f}{2} (F_{x,fr} - F_{x,fl}) + \frac{b_r}{2} (F_{x,rr} - F_{x,rl}) \right] \quad (20)$$

where I_z is the inertia moment in z-axis.

As the NTV has no roll stiffness of suspension, the roll motion of NTV can be presented as

$$\ddot{\theta} = \frac{1}{I_x + mh^2 \sin^2 \theta} \left[mhg \sin \theta - h \cos \theta \sum F_{y,ij} - mh^2 \dot{\theta}^2 \sin \theta \cos \theta - C_d \dot{\theta} \right] \quad (21)$$

where θ and $\dot{\theta}$ are the vehicle roll angle and roll rate, I_x is the vehicle roll moment of inertia, and C_d is the roll damping ratio of the suspension.

2.3 Simplified single-track vehicle model

The nonlinear equations of the four-wheel model provided in previous section are accurate and detailed in matching the real vehicle response. In controller design and performance analysis, a simplified single-track model has been delivered from the nonlinear equations (1)–(21). Assuming that the steer angle, side slip angle and roll angle approach zero at normal states, their sinusoidal value can be approximated to their own value using the small-angle approximation for simplification. And assume that the COG is at the middle of the track and the difference between COG to the front and rear axles is zero, which gives $l_f = l_r$. Simplify the foundation torque of rear left and rear right wheels as T_r and add the torque differential value of rear wheels as a new input ΔT_r to the system. Then the vehicle model can be simplified to a function of system state x and control input u as

$$\dot{x} = f(x) + g(x) \cdot u \quad (22)$$

where

$$x = [v \ \beta \ \dot{\phi} \ \theta \ \dot{\theta}]^T, \quad u = [\delta T_r \Delta T_r]^T \quad (23)$$

$$f(x) = \begin{bmatrix} -\frac{2C_\gamma}{m}\beta^2 + \frac{2\lambda_\gamma}{m}\beta\theta \\ -\frac{2C_\gamma}{m}\frac{\beta}{v} + \frac{2\lambda_\gamma}{m}\frac{\theta}{v} - \dot{\phi} \\ -\frac{C_\gamma l^2}{2I_z}\frac{\dot{\phi}}{v} \\ \dot{\theta} \\ \frac{mgh - 2\lambda_\gamma h}{I_x}\theta - \frac{C_d}{I_x}\dot{\theta} + \frac{2C_\gamma h}{I_x}\beta - \frac{mh^2}{I_x}\dot{\theta}^2\theta \end{bmatrix} \quad (24)$$

$$g(x) = \begin{bmatrix} \frac{C_\gamma}{m}\beta & \frac{C_\gamma}{mv} & \frac{C_\gamma l\beta}{2I_z} & 0 & -\frac{C_\gamma h}{I_x} \\ \frac{1}{mR_r} & -\frac{\beta}{mv} & 0 & 0 & 0 \\ 0 & 0 & \frac{b_r}{I_z} & 0 & 0 \end{bmatrix}^T \quad (25)$$

including the linearised tyre lateral behaviour as equivalent cornering stiffness coefficient C_γ and camber stiffness coefficient λ_γ .

The system will finally converge to its steady state with a given trajectory. When the vehicle is turning in a circle with radius of R , the system steady state value can be approximately calculated as

$$\begin{cases} \beta_0 = l/2R \\ \dot{\phi}_0 = v/R \\ \theta_0 = v^2/gR \end{cases} \quad (26)$$

2.4 Virtual rider model

The virtual rider model is produced to simulate the reaction of a rider of NTV with two objective, one is to maintain the stability of vehicle to reduce the risk of falling down and the other is to follow the path of the target route [9, 37]. For experienced rider, the two control objectives can be achieved together to perform the optimised operation. However, the virtual rider model needs to be developed assuming the rider has no special skills and experience in operating an NTV [2, 16, 38]. A solution is to apply two control algorithms independently, one aims to maintain the roll angle of the vehicle and the other aims to track the path. Each control algorithm has only one control objective and will not communicate with each other to simulate the behaviour of a new rider to ride an NTV. Different with riding a bicycle that the rider can shift its own body to help lean the bicycle, the weight of NTV is much higher than the weight of a rider. Thus, the shift of rider's position is not considered in the virtual rider and only the steer angle and traction torque are controlled by the virtual rider.

The steer angle control will result in not only the roll stability but also the lateral dynamics. Because of this, the control algorithm of steer angle can be easily developed as the sum of two simple controllers, one tracking the roll angle θ and the other tracking the yaw rate $\dot{\varphi}$. In roll stability control, a proportional derivative (PD) control is applied to track the error of roll angle [3] as

$$\delta_1 = (k_{p2} + sk_{d2})(\theta_{\text{ref}} - \theta) \quad (27)$$

In the lateral trajectory tracking, the rider applies steering input to track the target yaw rates obtained from path. It is assumed that the steer angle is proportional with the path to be followed [3]. As the required response speed of lateral trajectory tracking is slower than that of roll stability control, a pseudo-derivative feedback (PDF) control is applied in the yaw rate tracking. Comparing with the traditional PI (D) control, the PDF control can reduce the effect of derivative feedforward action to avoid the transient impact to roll stability [39]. The lateral control is designed as

$$\delta_2 = \frac{k_{i1}}{s}(\dot{\varphi}_{\text{ref}} - \dot{\varphi}) - k_{p1}\dot{\varphi} \quad (28)$$

The final steer angle control input can be calculated with combining the two outputs together as

$$\delta = \delta_1 + \delta_2 \quad (29)$$

Apart from the steering control to maintain the roll stability and follow the path, the vehicle speed needs to be controlled by virtual rider via throttle to generate equivalent traction torque to the vehicle. The vehicle velocity control is implemented via a PI controller as

$$T_r = \left(k_{p3} + \frac{k_{i3}}{s}\right)(V_{\text{ref}} - v) \quad (30)$$

3. Design of drive assistance system

This section includes two designs. The first design is a nonlinear tilting controller which compensates the nonlinear behaviour of DTC under different vehicle

velocity and operating state. The second design is two torque vectoring controllers to assist the rider to maintain the roll dynamics of NTV in cornering based on steer angle and tilting compensator, respectively.

3.1 Nonlinear tilting controller design

In the nonlinear controller design, the first step is to linearise the relation between system input and output, which is called input-output linearisation. The roll angle equation can be rewritten as

$$\ddot{\theta} = L_f(x) + B(\theta)M_t \quad (31)$$

where

$$L_f(x) = \frac{1}{I_x + mh^2 \sin^2 \theta} \left[mhg \sin \theta - mh^2 \dot{\theta}^2 \sin \theta \cos \theta - h \cos \theta \left(2C_f \delta - 2C_f \tan^{-1} \left(\frac{l_f \dot{\phi} + V_y}{V_x} \right) + 2\lambda_f \theta + 2C_r \tan^{-1} \left(\frac{-l_r \dot{\phi} + V_y}{V_x} \right) + 2\lambda_r \theta \right) \right] \quad (32)$$

$$B(\theta) = \frac{1}{I_x + mh^2 \sin^2 \theta} \quad (33)$$

As $B(x) \neq 0$ if $I_x > 0$, the $B(x)$ is known as non-singular for nominal operating points and $B(x)^{-1}$ is achievable. The required tilting motion as control input can be designed as

$$M_t = B^{-1}(-L_f(x) + u_t) \quad (34)$$

where u_t is designed as the control input to the linearised system

$$u_t = k_1(\theta^* - \theta) - k_2 \dot{\theta} \quad (35)$$

and θ^* is the ideal roll angle calculated as a function of steering angle and vehicle speed as

$$\theta^* = \tan^{-1} \left(\frac{V^2 \delta}{(l_f + l_r)g} \right) \quad (36)$$

Choose $B_0 = B(\theta)|_{\theta=0}$ as the nominal control gain at rated value. The difference between $B(x)$ and B_0 will be seen as disturbance in the lumped perturbation. Define the perturbation terms as

$$\ddot{\theta} = \Psi(x) + B_0 M_t \quad (37)$$

where

$$\begin{aligned} \Psi(x) &= L_f(x) + (B(x) - B_0)M_t \\ B_0 &= \frac{1}{I_x} \end{aligned} \quad (38)$$

Assume the lumped perturbation will not change quicker than one time cycle. Calculate the perturbation term as

$$\hat{\Psi}(t) \approx \Psi(t-1) = \ddot{\theta}(t-1) - B_0 M_t(t-1) \quad (39)$$

The final control input is

$$M_t = B_0^{-1} \left[-\hat{\Psi} + k_1 \tan^{-1} \left(\frac{V_x^2 \delta / g}{l_f + l_r} \right) - k_1 \theta - k_2 \dot{\theta} \right] \quad (40)$$

Figure 9 shows the block diagram of the nonlinear control for tilting mechanism of NTV.

3.2 Torque vectoring controller design

3.2.1 Steering angle based torque vectoring (SATV)

The easiest design to compensate the counter steering behaviour when turning a vehicle is to set the vectoring torque of rear wheels proportionally to the derivative of steer angle as

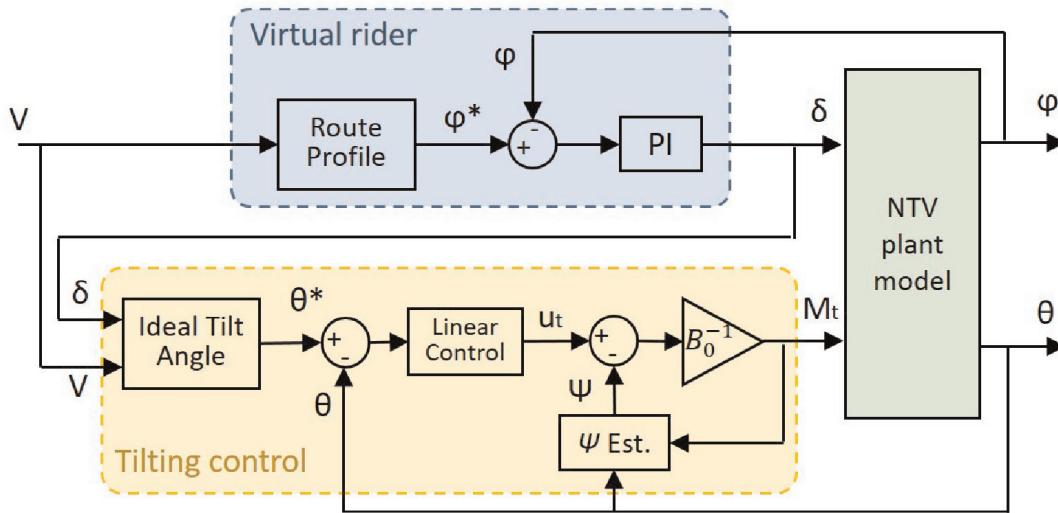


Figure 9. Control block diagram of the tilting control for the tilting mechanism of NTV.

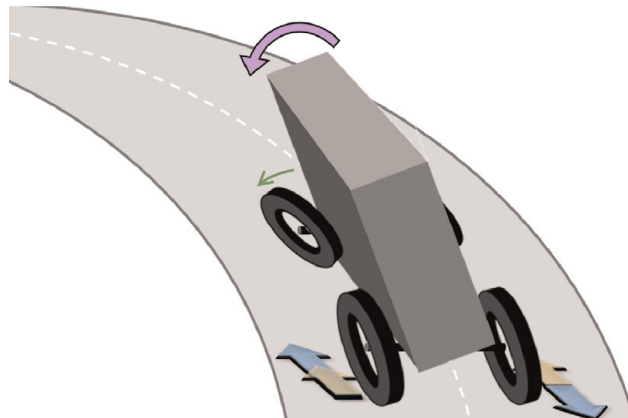


Figure 10. Vectoring torque assists the rider in balancing the NTV during a turn.

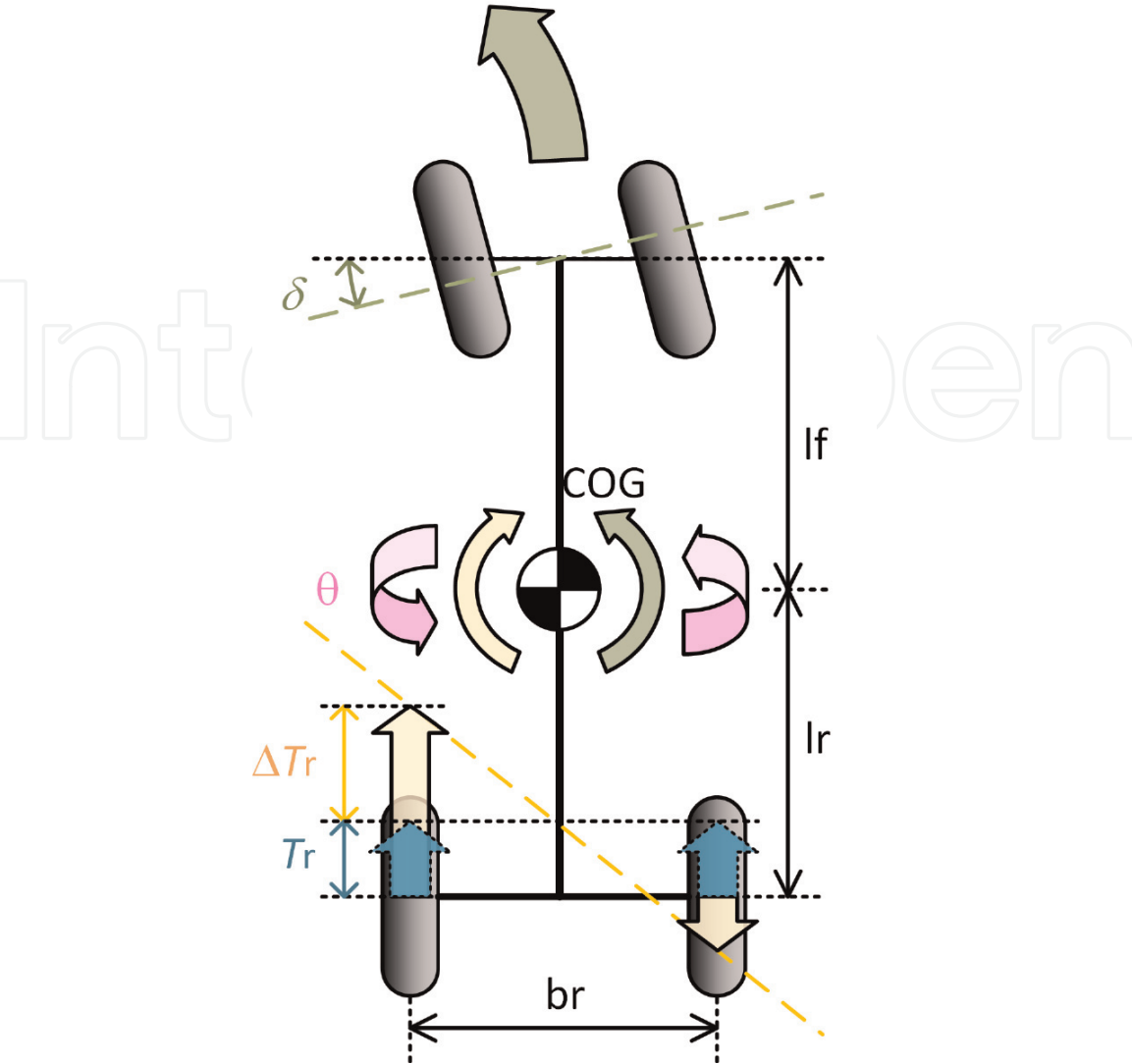


Figure 11.
 The diagram of torque vectoring for narrow tilting vehicle.

$$\Delta T_r = K\dot{\delta} \tag{41}$$

where K is the control gain designed to get expected performance. This parameter is chosen based on the bandwidth of the torque controller that its response speed have to be several times faster than yaw moment response speed and slower than torque response speed.

When the rider turning the vehicle, the torque controller activated the vectoring torque to yaw the vehicle in the opposite direction to lean the vehicle to the target position (**Figures 10** and **11**). With the drive assistance of vectoring torque, the rider is not required to act counter-steering to lean the vehicle manually.

3.2.2 Tilting compensator based torque vectoring (TCTV)

In steady-state that the vehicle keeps a unchanged states, $\ddot{\varphi}$ reaches zero and $\dot{\varphi}$ reaches its reference value. Then the steady-state steer angle can be obtained from the yaw dynamics in (22) as

$$\delta_{ss} = \frac{l}{v} \dot{\varphi} - \frac{2b_r}{C_r l} \Delta T_r \tag{42}$$

Substitute (42) into the roll dynamic equation in (22) to obtain:

$$\ddot{\theta} = \frac{1}{I_x} \left[(mgh - 2\lambda_\gamma h)\theta - C_d\dot{\theta} + 2C_\gamma h\beta - mh^2\dot{\theta}^2 - C_\gamma h \left(\frac{l}{v}\dot{\phi} - \frac{2b_r}{C_\gamma l} \Delta T_r \right) \right] \quad (43)$$

Assume $\dot{\theta}$ and $\ddot{\theta}$ are zero in steady state, one can obtain the equation below:

$$\ddot{\theta} = \frac{h}{I_x} \left[(mg - 2\lambda_\gamma)\theta + 2C_\gamma\beta - \frac{C_\gamma l}{v}\dot{\phi} + \frac{2b_r}{l} \Delta T_r \right] = \sigma \quad (44)$$

If design the control signal as

$$\sigma = \frac{h}{I_x} \frac{2b_r}{l} K\delta = K'\delta \quad (45)$$

the vectoring torque to improve roll stability can be obtained as

$$\Delta T_r = K\delta + \Psi \quad (46)$$

where

$$\Psi = \frac{l}{2b_r} [C_\gamma\delta - (mg - 2\lambda_\gamma)\theta - 2C_\gamma\beta] \quad (47)$$

Comparing (46) with (41), the additional component Ψ is defined as the tilting compensator (TC) to compensate the nonlinear impacts that could reduce the roll stability. The TC based torque vectoring (TCTV) method can manage the vectoring torque to reduce the counter steering during a turn. The block diagram of the TV based drive assistance system is shown in **Figure 12**.

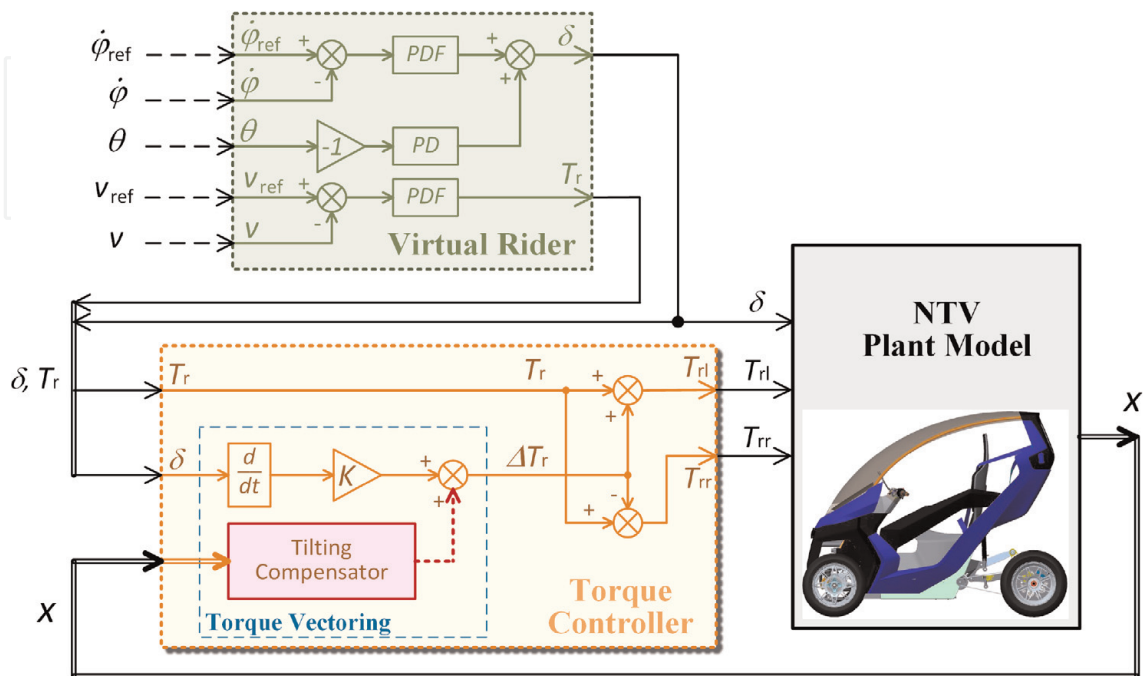


Figure 12.
The control block diagram of torque vectoring.

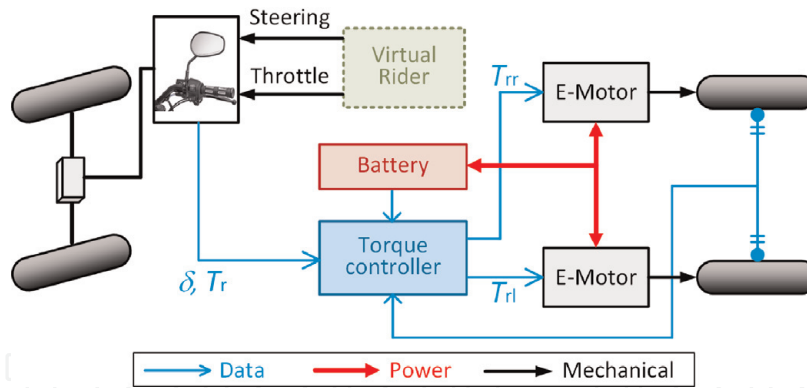


Figure 13.
 The data communication and power flow of torque vectoring in narrow tilting vehicle.

3.2.3 Torque management

For electric vehicles, the main source of vehicle propulsion is from the batteries. To protect the battery and electric motors from overload, the output power will be limited to manage the generated torque in the controller. The available torque applied to the motor can be described as

$$T_{avi} = \min \left(T_{m,rated}, \frac{\min (P_{m,rated}, P_{b,avi})}{\omega_m} \right) \quad (48)$$

where $T_{m,rated}$ and $P_{m,rated}$ is the rated torque and power of wheel motor; $P_{b,avi}$ is the maximum available output power from battery based on its current capacity. The final torque output can be managed as

$$T'_r = \min (T_r, T_{avi}) \quad (49)$$

$$\Delta T'_r = \min [\Delta T_r, (T_{avi} - T'_r)] \quad (50)$$

Then the final torque applied on the left and right rear wheels can be represented as

$$\begin{cases} T_{rl} = T'_r + \Delta T'_r \\ T_{rr} = T'_r - \Delta T'_r \end{cases} \quad (51)$$

The torque drive system of NTV is shown in **Figure 13**, where the data flow, electric power flow, and mechanical drive are given with blue, red and black arrows, respectively.

4. Simulation results

The following section verifies the designed controllers in assisting the rider to maintain the roll stability of the vehicle during a turn. The parameters of NTV are chosen from [1] and given in **Table 1**. The verification is based on the simulation in Matlab.

4.1 Result of nonlinear tilting control approach

4.1.1 Constant speed tilting test

The controllers used in simulation are with the parameters given in **Table 2**. The simulation validations of nonlinear tilting controller are carried out with tracking the

Description	Symbol	Value	Unit
Total vehicle mass	m	200.0	kg
Height of vehicle COG	h	0.5	m
Distance from COG to front axle	l_f	0.7	m
Distance from COG to rear axle	l_r	0.9	m
Length of track of front axle	b_f	0.5	m
Length of track of rear axle	b_r	0.7	m
Vehicle roll moment inertia	I_x	18	kg.m ²
Vehicle yaw moment inertia	I_z	80	kg.m ²
Front/Rear wheel radius	$R_{fj/rj}$	0.5	m
Front/Rear wheel rotational inertia	$J_{fj/rj}$	0.2	kg.m ²
Front cornering stiffness	C_f	3500	N/rad
Rear cornering stiffness	C_r	5480	N/rad
Front camber stiffness	λ_f	1000	N/rad
Rear camber stiffness	λ_r	2000	N/rad

Table 1.
System parameters of NTV.

Description	Symbol and value
Virtual rider	$K_p = 0.1, \quad K_i = 0.1$
Linear controller	$k_1 = 300, \quad k_2 = 400$
Gain-scheduling controller	$\begin{cases} k_1 = 300, \quad k_2 = 400 & (LS : v \leq 18 \text{ km/h}) \\ k_1 = 500, \quad k_2 = 1000 & (MS : 18 < v \leq 30 \text{ km/h}) \\ k_1 = 1500, \quad k_2 = 3000 & (HS : v > 30 \text{ km/h}) \end{cases}$
Nonlinear controller	$k_1 = 300, \quad k_2 = 400, \quad B_0 = 0.0556$

Table 2.
Control parameters.

route in a shape of ' ∞ '. The speed reference gives a constant and the yaw rate reference is in a square wave. The virtual rider maintains the vehicle yaw rate to track the predefined route path that is independent with the tilting controller. The route path tracking performance is shown in **Figure 14**, where the desired path is shown as the black line and the vehicle path is shown as the dashed red line. The vehicle path track is due to the yaw rate control of a virtual rider and the stability is controlled by the tilting mechanism. The entire control performance is good that the vehicle tracks the path well.

The vehicle yaw rate and roll angle performance at the constant speed of 20 km/h are shown as the simulation result in **Figure 15**. The yaw rate tracks the step changed reference by the virtual rider and the vehicle roll angle is controlled by the nonlinear tilting controller. The result in **Figure 15** compares between the control performance (blue line) and their reference (red dashed line). The result of roll angle tracking indicates that the controller is able to keep the vehicle stable during a turn.

4.1.2 Increasing and decreasing speed tilting test

In the increasing and decreasing speed tilting test, the same route path is employed for the validation with the varying vehicle velocity from low speed to

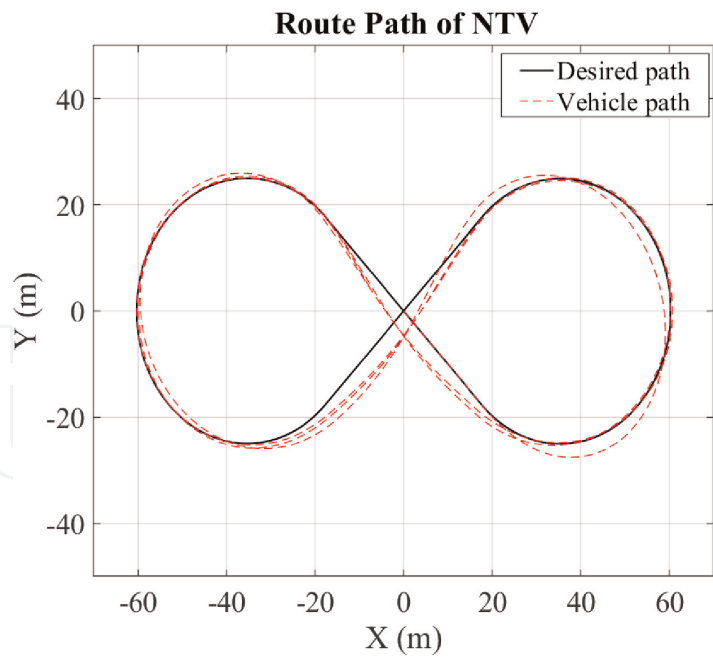


Figure 14.
Simulation result of vehicle route path tracking performance.

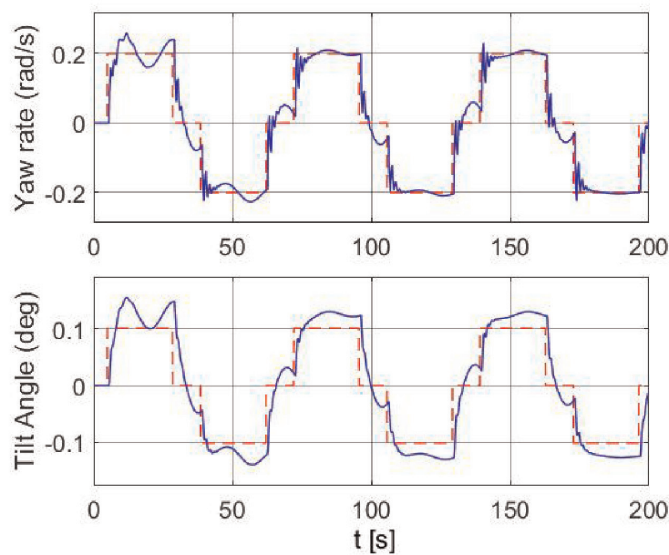


Figure 15.
Simulation result of vehicle yaw rate and roll angle at constant speed of 20 km/h.

high speed. With the change of vehicle speed, the reference yaw rate and roll angle are amended depending on the velocity. Its yawing and tilting dynamics have nonlinear behaviour under different speed. Three types of controller have been compared, the linear PI controller, the gain-scheduling PI controller, and the nonlinearity compensation based tilting controller.

The linear controller normally cannot perform well in the whole range of speed, especially at high vehicle speed. That is because the vehicle model includes high-order nonlinearities and the linear controller is designed based on the linearised model at a particular operating speed. Thus, the control performance can be guaranteed only at the target speed. The nonlinear effect, such as the variation of speed, will cause the controller difficult to maintain the optimised performance in the whole speed range.

To reduce the nonlinear effect at different operating speed, the gain-scheduling (GS) controller is to separate the whole speed region into small regions and the linear control law is applied in each region. When the vehicle velocity changed from low speed to high speed, the controller parameters switch among the predesigned regions to provide the desired control performance in the whole range of speed. The scheduled control parameters in three regions, low speed (LS), medium speed (MS) and high speed (HS), are given in **Table 2**. However, the switching between controllers reduces the control performance and the predefined controllers are not robust to the uncertainties in practice, including both the variation of vehicle parameters, such as the weight and COG of vehicle caused by the change of rider and passengers, and the environmental variation, such as the friction coefficient of road surface and impact of wind disturbance. As the simulation aims to verify the control algorithm under ideal condition, the impact of uncertainties is not presented in the simulation study.

The nonlinear controller is designed to cover the whole operating region from low vehicle velocity to high vehicle velocity. The structure of the nonlinear controller is the combination of a normal linear controller and a compensation block of estimated nonlinearity, as in **Figure 9**. The nonlinearity under different speed was compensated by the estimated nonlinear behaviour. The nonlinear approach improved the performance of tilting controller in the whole operating region.

In the chosen of controller parameters, the lower control gain can cause larger tracking error, while the higher control gain can cause more actuator usage and overshoots and can reduce the stability. The parameters of linear controller are chosen to minimise the roll angle tracking error in the whole operating range and, simultaneously, reduce the risk of causing unstable. To ensure a fair comparison, the GS control gain in each region is chosen by the method the same as that of the linear controller. And the nonlinear controller uses the same control gain as the linear controller additionally combined with the nonlinearity compensation block. The simulation results of vehicle yaw rate and roll angle controlled by the three controllers under the speed from 5 to 45 km/h are shown in **Figures 16–18**, respectively.

To verify the improvement of control performance numerically, the comparison among linear, gain-scheduling and nonlinear controllers is relied on the integral absolute error (IAE) of yaw rate and roll angle, as shown in **Figure 19**. All the three controllers are employed to control the same vehicle system with the same virtual rider model. The roll angle IAE of the nonlinear controller is 46% less than that of the GS controller and 75% less than that of the linear controller. In addition, the better performance the tilting controller acted on roll angle tracking, the easier the rider can maintain the vehicle in tracking the yaw rate.

With the same virtual rider, the performance of nonlinear controller has 24 and 9% less IAE in yaw rate tracking than that of the linear controller and GS controller, respectively. The results verified that the nonlinear tilting controller performs better in both maintaining the roll stability and tracking the lateral trajectory.

4.2 Result of torque vectoring approach

In the simulation validation, the TV controllers are applied to control the roll stability of NTV in tracking the route of a step yaw rate in two case studies. The first case is that the vehicle driven into a turn at a constant speed and the second case is that the vehicle accelerating during a turn. Both tests use the same rider model and vehicle plant model in the comparison among traditional controllers and proposed SATV and TCTV controllers. The parameter settings of the virtual rider model and torque controller are given in **Table 3**. The performance validates the effectiveness of the designed controller on counter steering reduction and the stability improvements of the designed controllers.

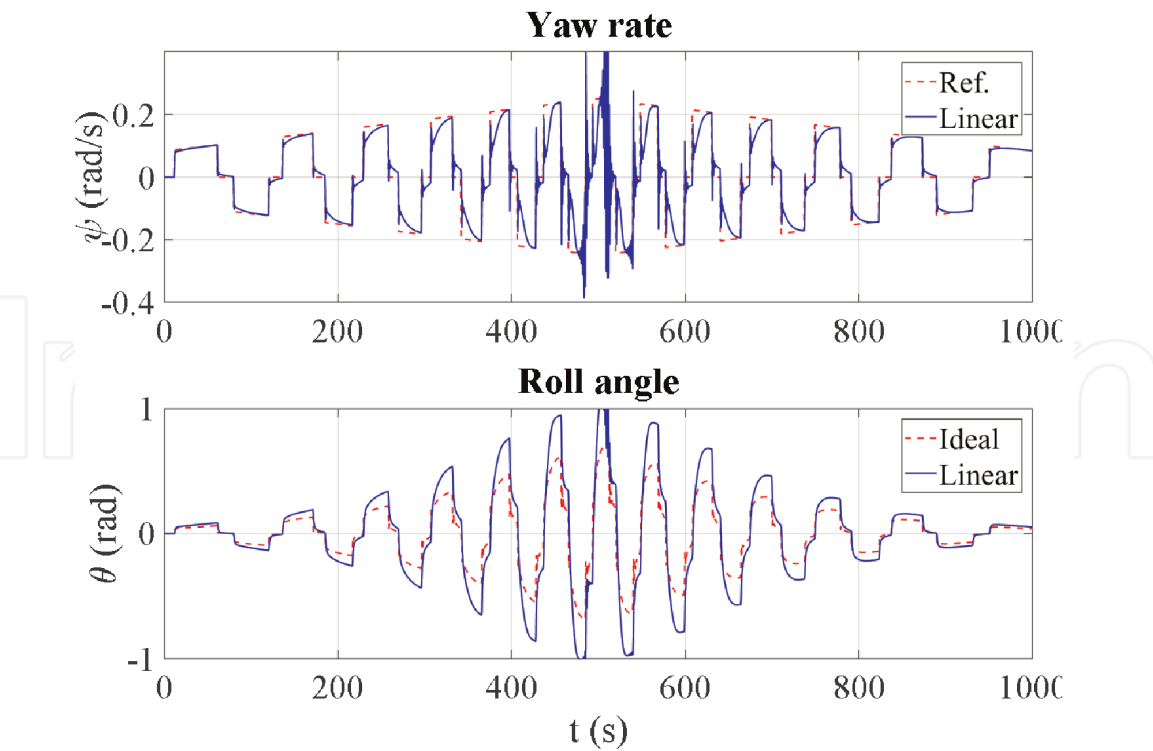


Figure 16.
Simulation result of yaw rate and roll angle with linear controller.

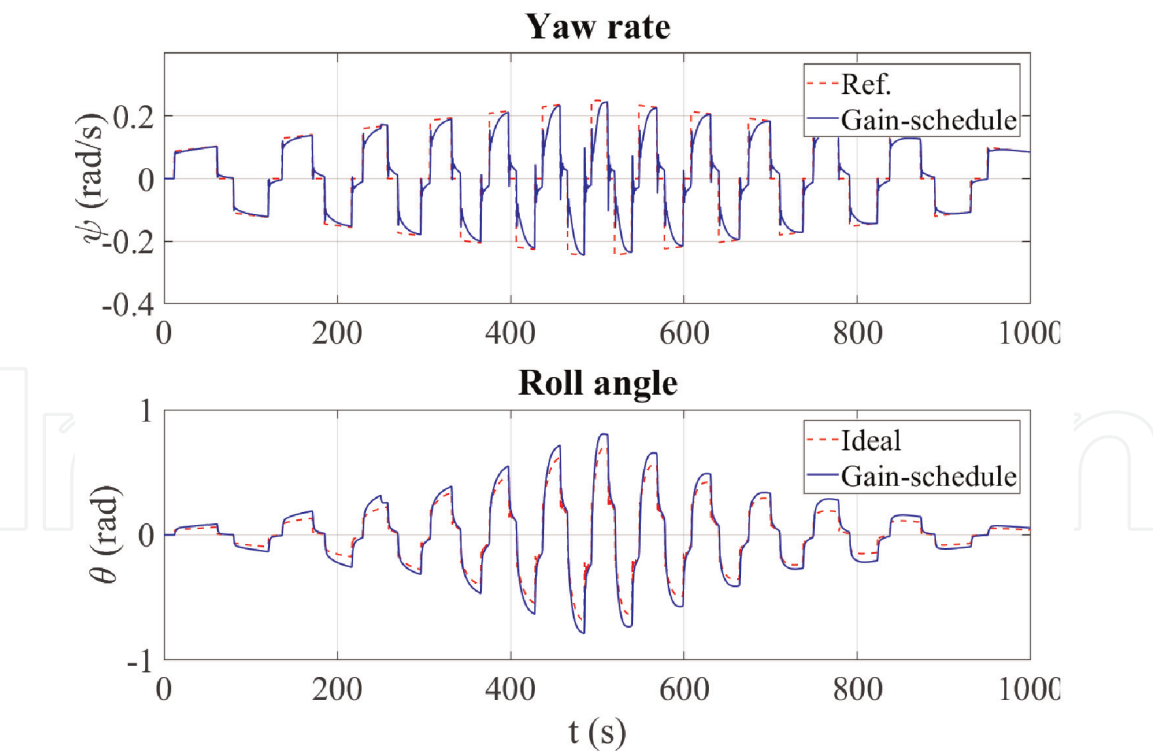


Figure 17.
Simulation result of yaw rate and roll angle with gain-scheduling controller.

4.2.1 Left turn under constant speed

The case study simulates the dynamic response of an NTV driving into a turn. The vehicle is driven straight with a constant speed of 5 m/s at first. Then the rider starts to turn the vehicle to track the path in a left turn with the radius of 15 m, as

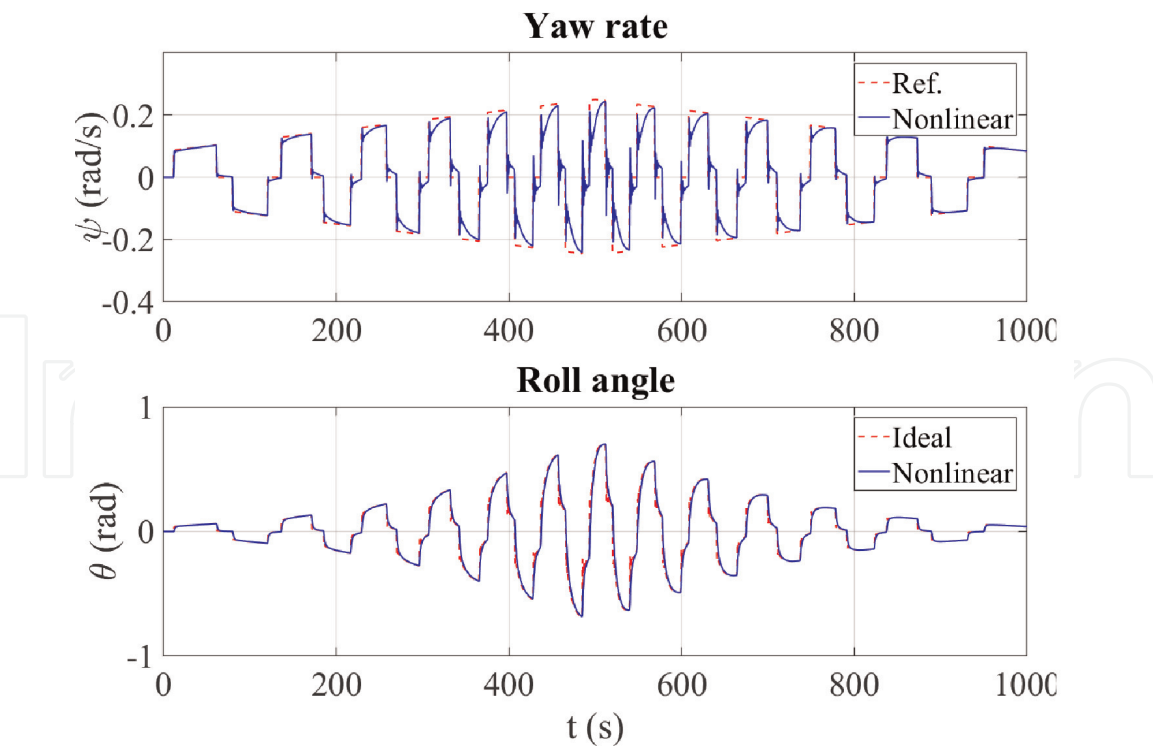


Figure 18.
Simulation result of yaw rate and roll angle with nonlinear controller.

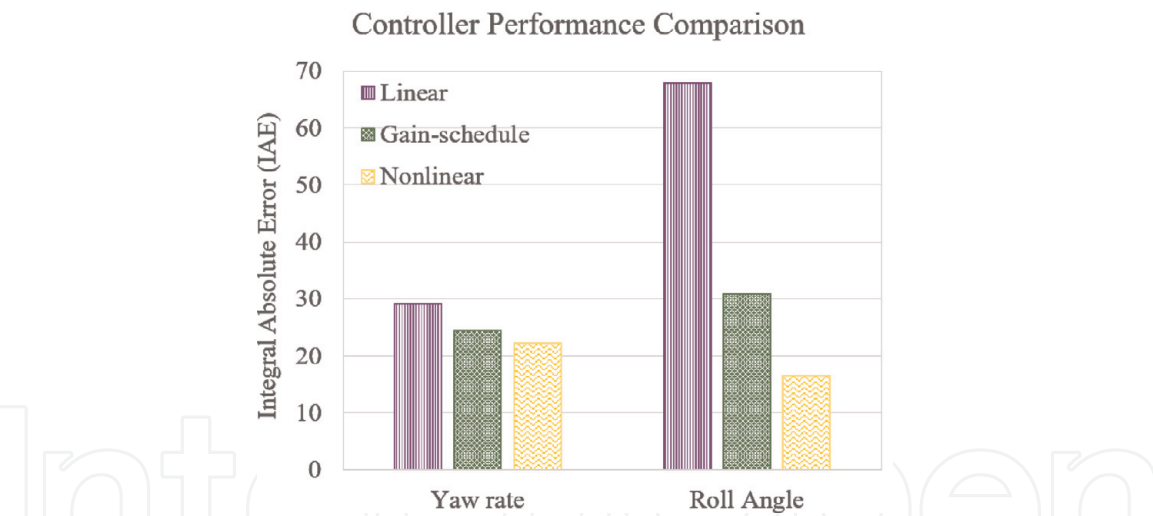


Figure 19.
Controller performance comparison among their IAE of yaw rate and roll angle.

Description	Symbol and value	
Virtual rider	$k_{p1} = 0.3$	$k_{i1} = 0.2$
	$k_{p2} = 1$	$k_{d2} = 5$
	$k_{p3} = 1$	$k_{i3} = 0.4$
Torque controller	$K = 50$	
	$T_{m, rated} = 50 \text{ Nm}$	
	$P_{m, rated} = 1500 \text{ W}$	

Table 3.
Controller parameter settings.

shown in **Figure 20**. The desired command to the virtual rider is a step changed yaw rate. The step change of yaw rate reference actually acts as a sudden disturbance to the torque controller to verify its transient response. In conventional method, the rider should counter-steer the front wheels to lean the vehicle into an opposite direction until the roll angle reaches the desired value to maintain its roll stability. With the assistance of torque vectoring, the requirements of counter-steer from rider will be reduced.

Figure 21 shows the dynamic response of the steering angle, vectoring torque, vehicle side-slip angle, yaw rate, lateral acceleration and roll rate. The comparisons are among the control inputs as well as the vehicle states performance under the control of the different controllers. Comparing the results, the requirements of counter-steering from rider have been eliminated in both the SATV and TCTV based control methods. Comparing between the two proposed TV methods, the TCTV has less oscillation than that of the SATV due to the tilting dynamics been compensated.

The steady state value of the target yaw rate is 19 deg/s and that of the side-slip angle is 2.9 deg, which can be calculated from (26). The yaw rate and lateral acceleration of the TCTV based torque control have less oscillation comparing with the other three methods. The steering angle is the main contributor to the performance of side-slip angle. This makes them to have the same response as shown in the results. Among the performances of all the controllers, the roll rate of the TCTV based torque control performs the best with the least peak tracking error and less oscillation.

The tracking error of all states is shown in **Figure 22** for a clearer comparison. In the comparison of tracking performance, the proposed controller performs better in transient response with less maximum tracking error and oscillation rate. The tracking error compensation speed is about 4 seconds to approach zero under disturbance. It verifies that both the transient stability and steady-state stability of roll dynamics can be maintained as desired with using the proposed controller.

The quantity comparison of maximum tracking error and integral absolute error (IAE) of each state is summarised and given in **Table 4**. With the usage of proposed TV controller, both the maximum tracking error and oscillation rate has been reduced comparing with traditional control method and normal TV approach. The TCTV eliminated the counter-steering process to ease the rider in operating the NTV and the maximum error of steering control is reduced about 74% comparing

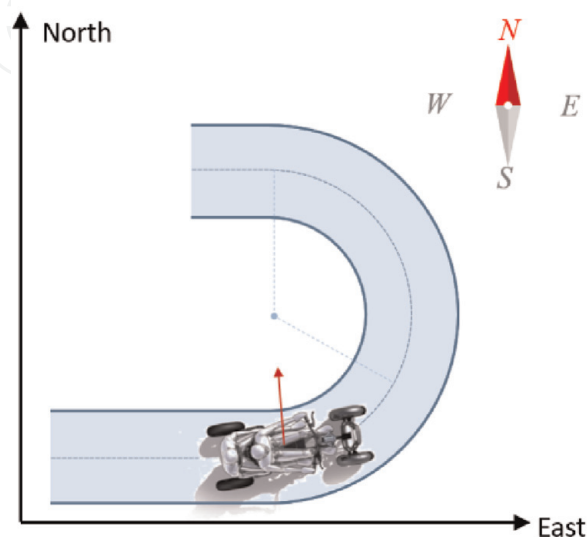


Figure 20.
Path of vehicle with left turn in simulation.

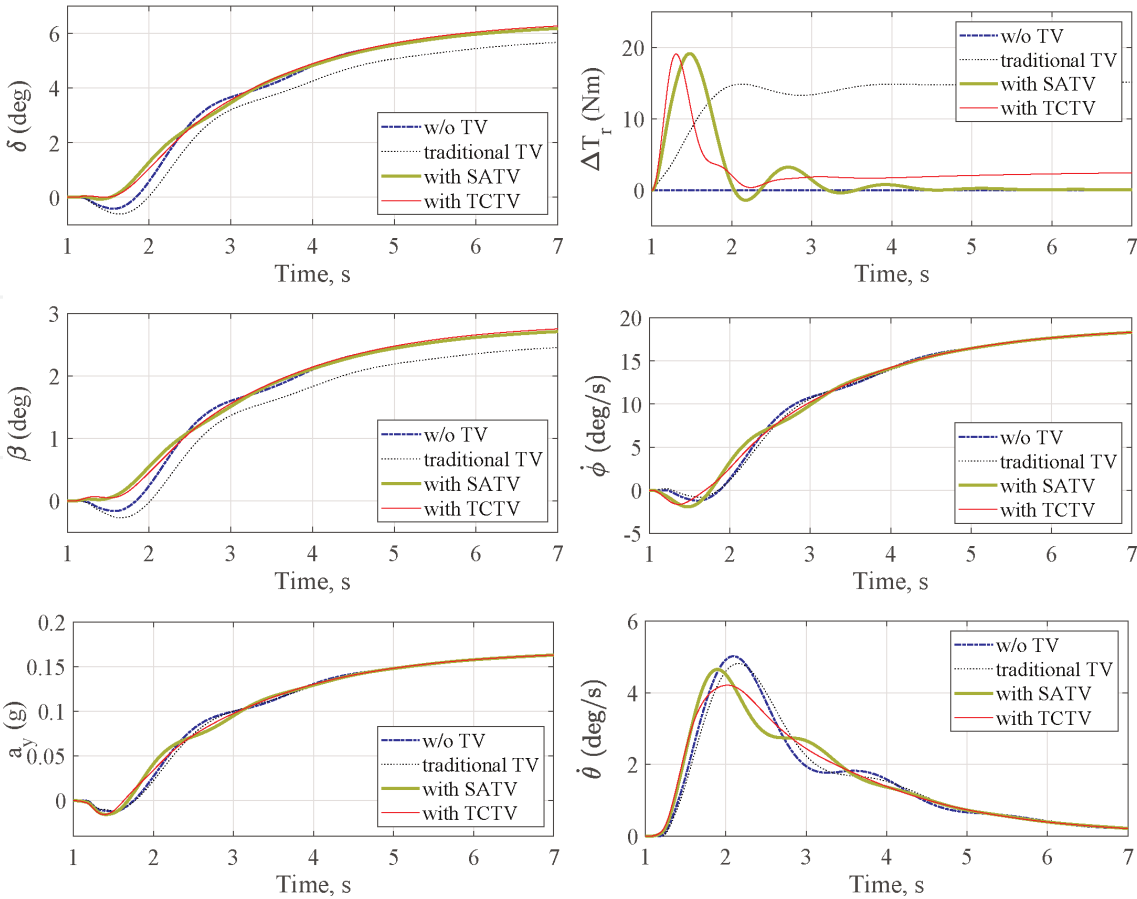


Figure 21.
Simulation result of case 1—left turn under constant speed.

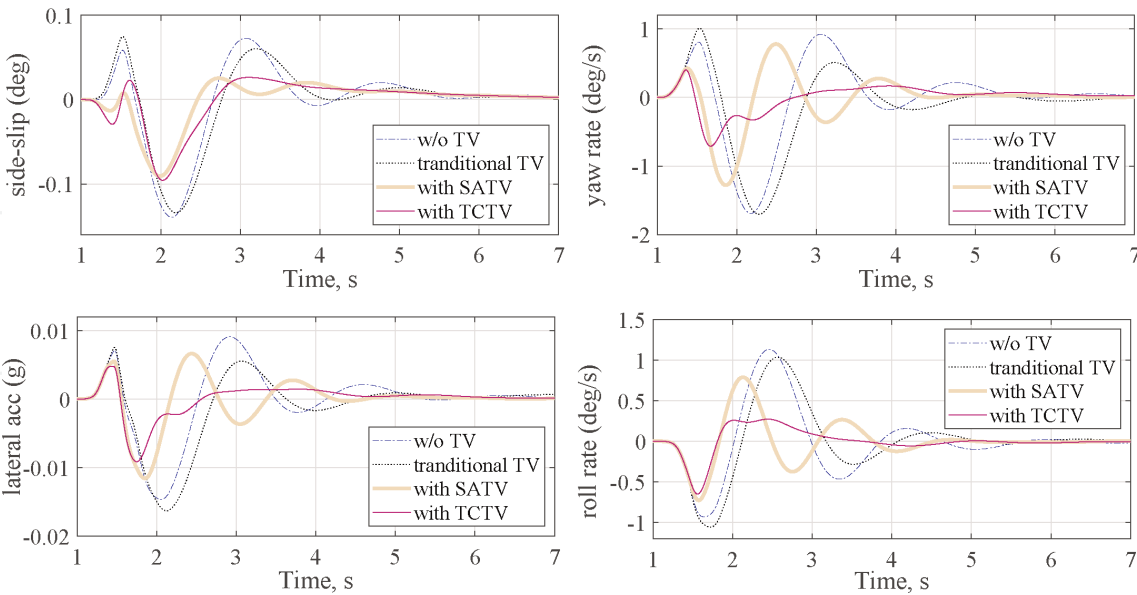


Figure 22.
States tracking error comparison of case 1.

with the result of conventional method. With the TCTV controller applied to the NTV, the side-slip angle, yaw rate, lateral acceleration, and roll rate have been improved with 35, 58, 36, 28% less maximum tracking error, respectively. To make the comparison more obvious, the indices of the maximum error, IAE and oscillation rate of all the control methods are shown in bar charts as in **Figure 23**.

Indices	Variables	w/o TV	Traditional TV	With SATV	With TCTV
Maximum track error	Counter-steer agl (deg)	0.553	0.311	0.107	0.006
	Side-slip agl (deg)	0.1442	0.138	0.0943	0.101
	Yaw rate (deg/s)	1.763	1.82	1.307	0.719
	Lateral acc ($\times 0.01$ m/s)	1.51	1.711	1.19	0.933
	Roll rate (deg/s)	1.166	1.086	0.803	0.653
Integral absolute error	Side-slip agl (deg-s)	0.297	0.290	0.160	0.185
	Yaw rate (deg)	3.66	3.43	2.07	1.24
	Lateral acc ($\times 0.01$ m/s)	3.136	3.217	1.861	1.199
	Roll rate (deg)	2.586	2.426	1.52	0.832
Oscillation rate	Counter-steer agl (%)	0.6093	0.6343	0.5442	0.5292
	Side-slip agl (%)	0.6807	0.7161	0.6082	0.5937
	Yaw rate (%)	0.4694	0.2709	0.2506	0.1829
	Lateral acc (%)	0.3912	0.205	0.1896	0.1217
	Roll rate (%)	3.691	2.123	1.947	1.546

Table 4.
Performance indices comparison among different controllers in turning at a constant speed.

4.2.2 Speed acceleration during a turn

In addition to the constant speed turn, the speed acceleration/deceleration will cause instability of the vehicle roll dynamics as well. The second case simulates the operating of NTV under the condition of speed accelerating during a turn. The initial state is the NTV driving at a constant speed of 5 m/s and turning left with a yaw rate of 5.8 deg/s in steady state. Then the rider increase the propulsion torque to accelerate the vehicle to test the response of the torque controller as well as the performance of the vehicle.

The dynamic response of an NTV is shown in **Figure 24** with two inputs and four system states. And the tracking error of all states is shown in **Figure 25**. The result in this case is similar to the previous one that both the SATV and TCTV reduced the requirements of counter-steering from rider and improves the roll stability with less tracking error. In the yaw rate and roll rate comparison, the TCTV performs the best with the least peak error and fastest response time. The numerical results and bar chart comparison of the maximum tracking error, IAE and oscillation rate are given in **Table 5** and **Figure 26**. The TCTV method reduced the maximum tracking error in steer angle, side-slip, yaw rate, lateral acceleration and roll rate with 35%, 44%, 59%, 73% and 55% less value, respectively.

The cases aim to verify the control performance of developed torque controller in sudden turning and speed acceleration during a turn. These two cases verifies the vehicle stability with the proposed torque controller under sudden disturbance and time-varying disturbance, respectively. In both cases, the counter steering requirements can be fully eliminated and the maximum tracking error and oscillation rate of state tracking performance can be reduced for the average of 1/3 with using the proposed TV approach. Comparing the two cases, the improvement is more obvious

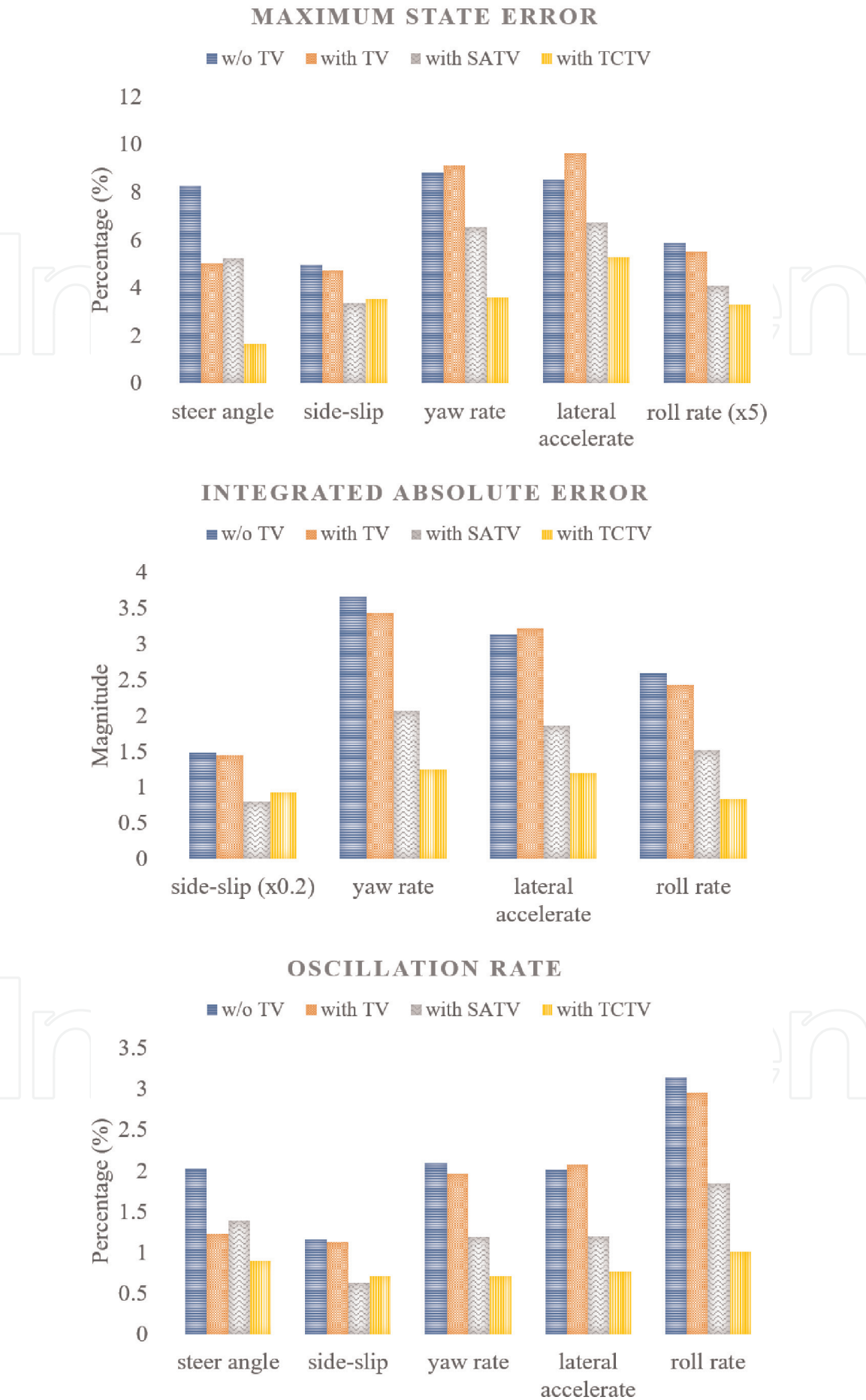


Figure 23.
The performance indices comparison among different torque controllers in the turning.

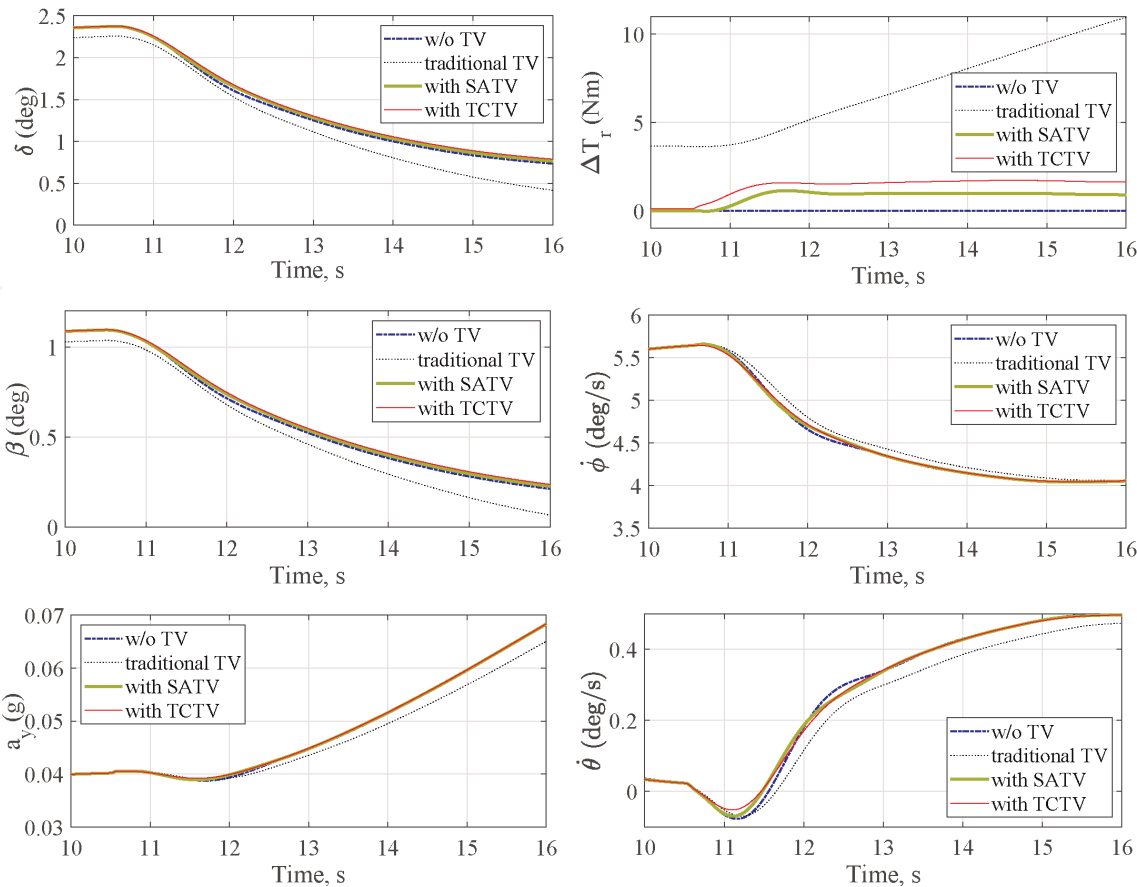


Figure 24.
Simulation result of case 2—acceleration during a turn.

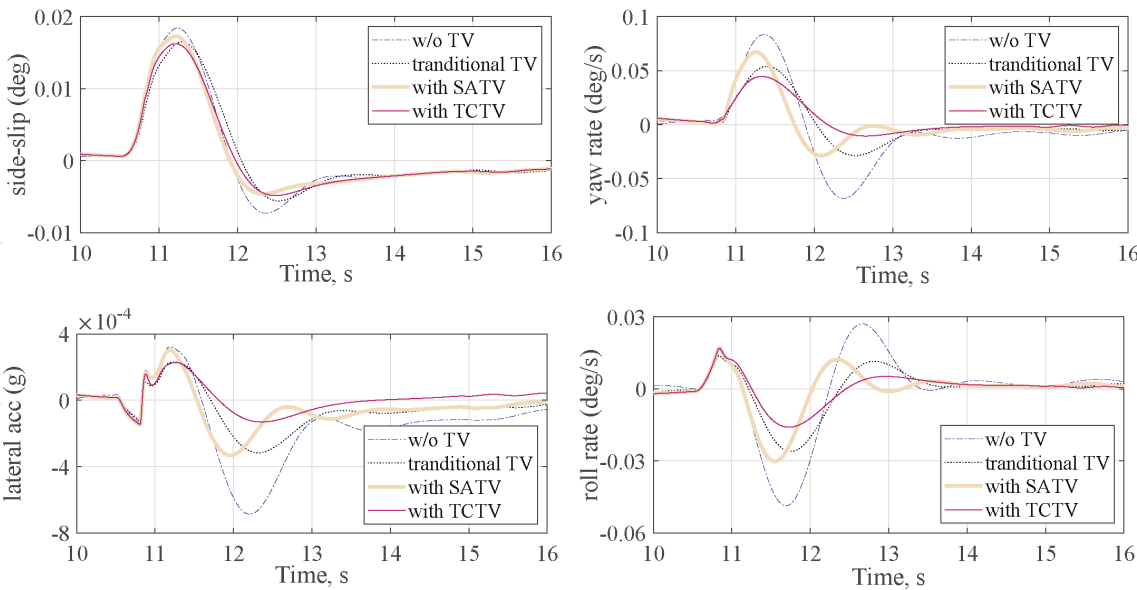


Figure 25.
States tracking error comparison of case 2.

in speed acceleration during a turn as it is more suitable for the time-varying disturbance on roll stability. Therefore, the NTV equipped with the drive assistance system will be easy to be ridden by any types of riders from new to experienced ones.

Indices	Variables	w/o TV	Traditional TV	With SATV	With TCTV
Maximum track error	Counter-steer agl (deg)	0.053	0.013	0.0027	0
	Side-slip agl (deg)	0.0184	0.0165	0.0173	0.0162
	Yaw rate (deg/s)	0.0834	0.0539	0.0673	0.0447
	Lateral acc ($\times 0.01$ g)	0.0687	0.0316	0.0332	0.0229
	Roll rate (deg/s)	0.049	0.0261	0.0302	0.0169
Integral absolute error	Side-slip agl (deg-s)	0.0266	0.0246	0.0242	0.0239
	Yaw rate (deg)	0.137	0.0793	0.0733	0.0535
	Lateral acc ($\times 0.01$ m/s)	0.118	0.0619	0.0572	0.0367
	Roll rate (deg)	0.0628	0.0332	0.0263	0.0361
Oscillation rate	Counter-steer agl (%)	0.6093	0.6343	0.5442	0.5292
	Side-slip agl (%)	0.6807	0.7161	0.6082	0.5937
	Yaw rate (%)	0.4694	0.2709	0.2506	0.1829
	Lateral acc (%)	0.3912	0.205	0.1896	0.1217
	Roll rate (%)	3.691	2.123	1.947	1.546

Table 5.
Performance indices comparison among different controllers in accelerating in a turn.

However, one limitation of this work is that it only simulated the driving assistant system in NTV under ideal condition, more uncertainty impact as well as the experimental verification can be done in future work. In addition, only two tilting state have been considered in the controller design and verification, turning with a constant speed and speed changes in a turn. The future research will also focus on other tilting states that are more complicated and challenged, such as maintaining the stability of NTV at highsider to avoid following down.

5. Conclusions

This chapter has reviewed the wheel and vehicle models of NTV and designed a nonlinear tilting controller for DTC-based mechanisms and two torque vectoring based drive assistance systems for torque control to help the rider in balancing the NTV during a turn. The nonlinear tilting controller has the capability to compensate the nonlinearities of vehicle tilting dynamics without the accurate vehicle model and been validated in simulation by comparing with the linear and gain-scheduling control approaches. The nonlinear tilting controller reduced the nonlinear tracking performance at different vehicle velocities and improved the yaw rate tracking performance as indicated in the results. The designed SATV and TCTV torque controllers are validated with the same vehicle model and compared with the traditional TV approach. The proposed controllers eliminated the counter-steering and improved the roll stability in balancing the vehicle. The peak tracking error, IAE and oscillation rate have been reduced by the tilting compensator and the vehicle dynamics are easier to be stable. Thus, the designed drive assistance systems can help riders with different experiences to balance the vehicle when driving an NTV.

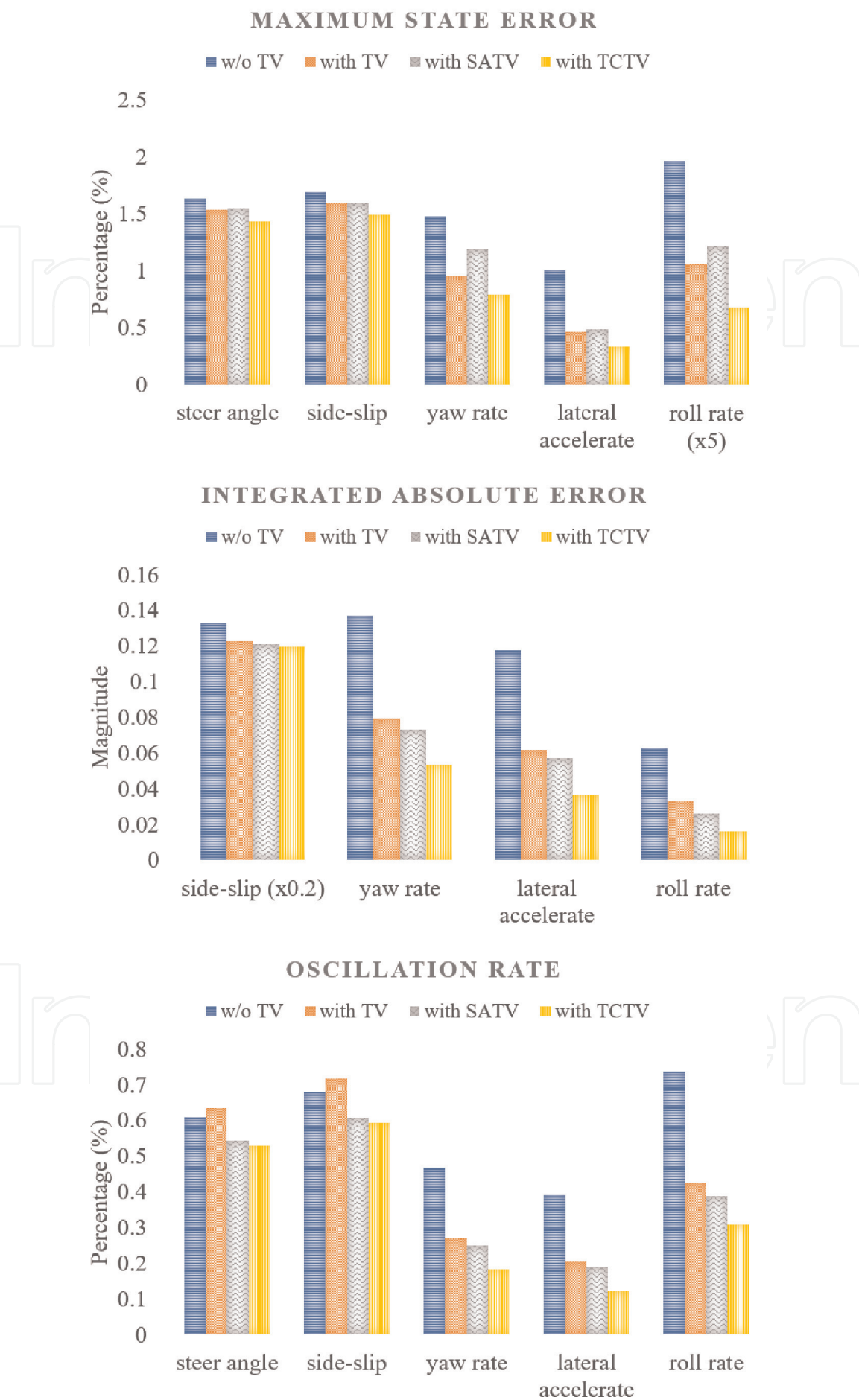


Figure 26.
The performance indices comparison among different torque controllers when accelerating in a turn.

Acknowledgements

The research presented in this chapter was undertaken as part of the Range of Electric Solutions for L Category Vehicles (RESOLVE) Project. Funded through the European Funding for Research and Innovation (Horizon 2020), Grant Number 653511.

IntechOpen


IntechOpen

Author details

Yaxing Ren
University of Warwick, Coventry, UK

*Address all correspondence to: yaxing.ren@warwick.ac.uk

IntechOpen

© 2020 The Author(s). Licensee IntechOpen. Distributed under the terms of the Creative Commons Attribution - NonCommercial 4.0 License (<https://creativecommons.org/licenses/by-nc/4.0/>), which permits use, distribution and reproduction for non-commercial purposes, provided the original is properly cited. 

References

- [1] Gohl J, Rajamani R, Starr P, Alexander L. Development of a novel tilt-controlled narrow commuter vehicle. Minnesota, Minneapolis, MN, USA: Department of Mechanical Engineering University Reports CTS 06-05; 2006
- [2] Kidane S, Alexander L, Rajamani R, Starr P, Donath M. Road bank angle considerations in modeling and tilt stability controller design for narrow commuter vehicles. In: American Control Conference. Minneapolis, MN, USA: IEEE; 2006. p. 6
- [3] Van Poelgeest A. The dynamics and control of a three-wheeled tilting vehicle [PhD thesis]. University of Bath; 2011
- [4] Robertson J. Active Control of Narrow Tilting Vehicle Dynamics [PhD thesis]. Bath, UK: University of Bath; 2014
- [5] Berote JJH. Dynamics and Control of a Tilting Three Wheeled Vehicle. Ph.D. dissertation. Bath, UK: University of Bath; 2010
- [6] Ren Y, Dinh Q, Marco J, Greenwood D, Hesar C. Nonlinearity compensation based tilting controller for electric narrow tilting vehicles. In: 2018 5th International Conference on Control, Decision and Information Technologies (CoDIT). Thessaloniki, Greece: IEEE; 2018. pp. 1085-1090
- [7] Ren Y, Dinh Q, Marco J, Greenwood D. Torque vectoring-based drive: Assistance system for turning an electric narrow tilting vehicle. Proceedings of the Institution of Mechanical Engineers, Part I: Journal of Systems and Control Engineering. 2019;233(7):788-800. DOI: 10.1177/0959651818823589
- [8] RESOLVE Project. 2018. Available from: <http://www.resolve-project.eu/>
- [9] Fajans J. Steering in bicycles and motorcycles. American Journal of Physics. 2000;68(7):654-659
- [10] Fabien C, Ph C, Lama M. Non-linear control of a narrow tilting vehicle. In: 2014 IEEE International Conference on Systems, Man and Cybernetics (SMC). San Diego, CA, USA: IEEE; 2014. pp. 2488-2494
- [11] Pojani D, Stead D. Sustainable urban transport in the developing world: Beyond megacities. Sustainability. 2015; 7(6):7784-7805
- [12] Li L, Lu Y, Wang R, Chen J. A three-dimensional dynamics control framework of vehicle lateral stability and rollover prevention via active braking with MPC. IEEE Transactions on Industrial Electronics. 2017;64(4):3389-3401
- [13] Snell A. An active roll-moment control strategy for narrow tilting commuter vehicles. Vehicle System Dynamics. 1998;29(5):277-307
- [14] Mourad L, Claveau F, Chevrel P. Direct and steering tilt robust control of narrow vehicles. IEEE Transactions on Intelligent Transportation Systems. 2014;15(3):1206-1215
- [15] Van Den Brink CR, Kroonen HM. DVC¹—The banking technology driving the CARVER vehicle class. In: 2004 7th International Symposium on Advanced Vehicle Control. Arnhem, The Netherlands; 2004
- [16] Kidane S, Alexander L, Rajamani R, Starr P, Donath M. A fundamental investigation of tilt control systems for narrow commuter vehicles. Vehicle System Dynamics. 2008;46(4):295-322
- [17] So S-G, Karnopp D. Active dual mode tilt control for narrow ground vehicles. Vehicle System Dynamics. 1997;27(1):19-36
- [18] Chiou J-C, Chen C-L. Modeling and verification of a diamond-shape narrow-tilting vehicle. IEEE/ASME Transactions on Mechatronics. 2008;13(6):678-691

- [19] Furuichi H, Huang J, Fukuda T, Matsuno T. Switching dynamic modeling and driving stability analysis of three-wheeled narrow tilting vehicle. *IEEE/ASME Transactions on Mechatronics*. 2014;**19**(4):1309-1322
- [20] Piyabongkarn D, Keviczky T, Rajamani R. Active direct tilt control for stability enhancement of a narrow commuter vehicle. *International Journal of Automotive Technology*. 2004;**5**(2): 77-88
- [21] Mourad L, Claveau F, Chevrel P. Design of a two DOF gain scheduled frequency shaped LQ controller for narrow tilting vehicles. In: *American Control Conference (ACC) IEEE*. 2012. pp. 6739-6744
- [22] De Novellis L, Sorniotti A, Gruber P. Wheel torque distribution criteria for electric vehicles with torque-vectoring differentials. *IEEE Transactions on Vehicular Technology*. 2014;**63**(4): 1593-1602
- [23] Sawase K, Sano Y. Application of active yaw control to vehicle dynamics by utilizing driving/breaking force. *JSAE Review*. 1999;**20**(2):289-295
- [24] Sawase K, Ushiroda Y, Miura T. Left-right torque vectoring technology as the core of super all wheel control (S-AWC). *Mitsubishi Motors Technical Review*. 2006;**18**:16-23
- [25] Sawase K, Ushiroda Y. Improvement of vehicle dynamics by right-and-left torque vectoring system in various drivetrains. *Mitsubishi Motors Technical Review*. 2008;**20**:14
- [26] Kang J, Heo H, et al. Control Allocation Based Optimal Torque Vectoring for 4WD Electric Vehicle. Technical Report, SAE Technical Paper. SAE International; 2012
- [27] Yim S, Choi J, Yi K. Coordinated control of hybrid 4WD vehicles for enhanced maneuverability and lateral stability. *IEEE Transactions on Vehicular Technology*. 2012;**61**(4): 1946-1950
- [28] Fallah S, Khajepour A, Fidan B, Chen S-K, Litkouhi B. Vehicle optimal torque vectoring using state-derivative feedback and linear matrix inequality. *IEEE Transactions on Vehicular Technology*. 2013;**62**(4):1540-1552
- [29] Her H, Koh Y, Joa E, Yi K, Kim K. An integrated control of differential braking, front/rear traction, and active roll moment for limit handling performance. *IEEE Transactions on Vehicular Technology*. 2016;**65**(6): 4288-4300
- [30] Koehler S, Viehl A, Bringmann O, Rosenstiel W. Energy-efficiency optimisation of torque vectoring control for battery electric vehicles. *IEEE Intelligent Transportation Systems Magazine*. 2017;**9**(3):59-74
- [31] Hibbard R, Karnopp D. Twenty first century transportation system solutions-a new type of small, relatively tall and narrow active tilting commuter vehicle. *Vehicle System Dynamics*. Taylor & Francis; 1996; **25**(5):321-347
- [32] So S-G, Karnopp D. Switching strategies for narrow ground vehicles with dual mode automatic tilt control. *International Journal of Vehicle Design*. 1997;**18**(5):518-532
- [33] Rajamani R, Gohl J, Alexander L, Starr P. Dynamics of narrow tilting vehicles. *Mathematical and Computer modelling of Dynamical Systems*. 2003; **9**(2):209-231
- [34] Kumar P, Merzouki R, Conrard B, Coelen V, Ould Bouamama B. Multilevel modeling of the traffic dynamic. *IEEE Transactions on Intelligent Transportation Systems*. 2014;**15**(3): 1066-1082

[35] Pacejka H. Tire and Vehicle Dynamics. 2nd ed. London, UK: Butterworth-Heinemann, Elsevier; 2005

[36] Svendenius J. Tire modeling and friction estimation [PhD theses]. 2007

[37] Ruggero F, Alessandro B. A virtual motorcycle driver for closed-loop simulation. IEEE Control Systems. 2006;**26**(5):62-77

[38] Kidane S, Rajamani R, Alexander L, Starr PJ, Donath M. Development and experimental evaluation of a tilt stability control system for narrow commuter vehicles. IEEE Transactions on Control Systems Technology. IEEE; 2010;**18**(6): 1266-1279

[39] Ohm DY. Analysis of pid and pdf compensators for motion control systems. In: Industry Applications Society Annual Meeting, Conference Record of the 1994 IEEE. Vol. 2. 1994. pp. 1923-1929